Time-to-space conversion of ultrafast waveforms at 1.55 μm in a planar periodically poled lithium niobate waveguide

Dror Shayovitz,[1,*] Harald Herrmann,[2] Wolfgang Sohler,[2] Raimund Ricken,[2] Christine Silberhorn,[2] and Dan M. Marom[1]

[1]*Department of Applied Physics, Hebrew University of Jerusalem, Jerusalem 91904, Israel*

[2]*Applied Physics, University of Paderborn, Warburger Str. 100, D-33098 Paderborn, Germany*

**Corresponding author: dror.shayovitz@mail.huji.ac.il*

Received August 16, 2013; revised October 9, 2013; accepted October 9, 2013; posted October 10, 2013 (Doc. ID 195946); published November 12, 2013

We report the first demonstration, to our knowledge, of time-to-space conversion of subpicosecond pulses in a slab nonlinear waveguide. By vertically confining the nondegenerate sum-frequency generation interaction between a spatially dispersed 100 fs signal pulse at 1.55 μm and a reference pulse in a titanium indiffused planar periodically poled lithium niobate crystal waveguide, we have attained a conversion efficiency of 0.1% and a conversion efficiency slope of 4% per watt of reference beam power. This was achieved while maintaining high conversion resolution, with a measured time window of operation of 48 ps resulting in a serial-to-parallel demultiplexing factor of 90.

OCIS codes: (190.0190) Nonlinear optics; (320.0320) Ultrafast optics; (060.0060) Fiber optics and optical communications.

http://dx.doi.org/10.1364/OL.38.004708

The continued rapid growth in Internet and data center traffic stimulates research into optical communications transmission techniques, in order to increase data capacity and spectral efficiency and reduce energy consumption. Optical time division multiplexing (OTDM) enables generation of record multi-Tbaud symbol rates on a single wavelength channel, and can be combined with advanced modulation formats to achieve greater than 10 Tb/s data transmission [1]. Techniques for demultiplexing a Tb/s OTDM channel must exploit optical nonlinearities due to the limited bandwidth (up to around 100 GHz) of optoelectronic devices. Various types of all-optical switching to extract a single bit from an OTDM channel have been investigated, including the nonlinear optical loop mirror [2,3], sum-frequency generation (SFG) in periodically poled lithium niobate (PPLN) waveguides [4], and four-wave mixing (FWM) in silicon and chalcogenide nonlinear waveguides [5,6]. However, the number of switching devices required scales with the OTDM symbol rate, increasing the total power consumption and system complexity.

Serial-to-parallel demultiplexing methods overcome this problem by using a single device to simultaneously demultiplex an entire OTDM channel, on a frame-by-frame basis. Examples include multiple quantum well based time-to-space (T-S) conversion [7], time-to-frequency conversion by FWM [8,9], and spectrally resolved SFG T-S conversion [10–16]. T-S conversion transforms the OTDM serial pulse stream into a quasi-static parallel spatial image, using SFG between multiple signal pulses and a single reference pulse. Each output spatial pulse image corresponds to a single OTDM bit slot and so may be directly detected by a photodetector or mixed with a narrow linewidth local oscillator for coherent detection.

T-S conversion by degenerate SFG was first demonstrated at 920 nm with an LBO nonlinear crystal [10] and later at 1550 nm with bulk PPLN [13]. We have previously performed background-free T-S conversion using nondegenerate and collinearly phase-matched SFG in a BBO crystal [14] and in bulk PPLN [15]. However, free-space diffraction of the signal and reference beams in the bulk nonlinear crystal limits the SFG interaction length, and therefore also limits the T-S conversion efficiency. To achieve reasonable conversion efficiencies, a high-peak-power (some hundreds of kilowatts) reference pulse is needed, making the T-S conversion technique impractical for real system use. In order to overcome this barrier, it is necessary to both increase the intensity of the interacting beams by tight focusing and simultaneously increase the interaction length. In the free-space regime, tighter focusing results in more rapid beam spreading due to diffraction and therefore reduced interaction length. However, confinement of the SFG interaction in a nonlinear planar waveguide prevents beam spreading in one dimension and thus a greater effective interaction length can be achieved.

In this Letter, we report the first demonstration, to our knowledge, of T-S conversion in a planar nonlinear waveguide [16]. By confining the interacting signal and reference light within a PPLN slab waveguide, we have significantly improved the T-S conversion efficiency compared to our previous work in bulk PPLN [15], while maintaining a high serial-to-parallel demultiplexing factor.

The operation of a T-S processor is described in detail in [10–12] and briefly summarized here. The signal pulse stream and a single reference pulse are incident on diffraction gratings and pass through Fourier lenses, such that their resolved frequency components are superimposed at the spectral plane with equal magnitudes but opposite directions of the spatial dispersions. By placing a $\chi^{(2)}$ nonlinear crystal at the spectral plane, SFG between the superimposed frequency components occurs at each point in space. Due to the matched yet flipped spatial dispersions, a quasi-monochromatic SFG wave is generated across the crystal aperture. The SFG light carries an instantaneous linear spatial phase, which is

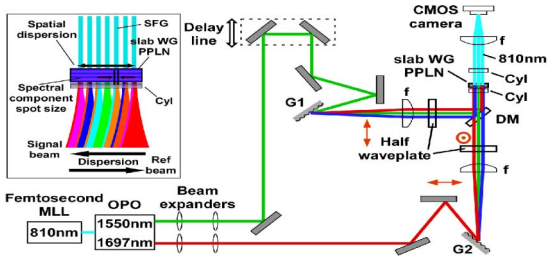

Fig. 1. Experimental setup (MLL, mode-locked laser; OPO, optical parametric oscillator; G1/G2, grating; f, Fourier lens; Cyl, vertical cylindrical lens; DM, dichroic mirror; slab WG PPLN, slab waveguide in PPLN). Inset: dispersed signal and reference beams at the slab WG PPLN.

directly dependant on the time delay between the incoming signal and reference pulses. A second Fourier lens placed after the crystal converts this instantaneous linear phase into a transverse spatial shift of the focused pulse image at the output plane. The result is a slowly varying spatial image of the input signal waveform with one-to-one mapping of the temporal position of the incoming pulses to the spatial position of the output image.

Figure 1 shows the slab waveguide PPLN T-S experimental setup. The signal and idler (reference) pulses of a spectra-physics opal optical parametric oscillator (OPO) have central wavelengths of 1550 and 1697 nm, respectively, FWHM pulse durations of 100 and 210 fs, respectively, and an 80 MHz repetition rate. The two beams are anamorphically expanded to appropriate collimated beam sizes in the vertical and horizontal directions and undergo equal and opposite linear spatial dispersions of approximately 5 mm over a 40 nm (–3 dB) bandwidth by diffraction gratings and 75 mm Fourier lenses. The dispersed beams are then superimposed by a dichroic mirror and focused in the vertical direction with a 6.4 mm cylindrical lens. This focal length was chosen to try to obtain best mode matching between the free-space vertically focused mode sizes at the input facet of the PPLN slab waveguide to the guided mode size within the waveguide.

The PPLN chip (with length 4 mm; see Fig. 2) was positioned along the optical axis such that the dispersed signal and reference beams' horizontal spectral planes were located at its center, in order to best exploit the waveguide length for generation of SFG light. The cylindrical focusing lens was then placed such that the signal and reference beams' vertical focal planes were displaced

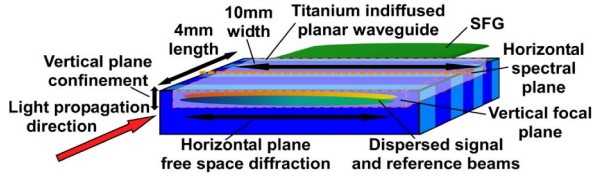

Fig. 2. Slab waveguide PPLN (not to scale) showing titanium indiffusion defined waveguiding region, spatially dispersed signal and reference beams vertically focused to the waveguide entrance facet and horizontally focused to the center of the crystal, and SFG light at the output facet.

by 2 mm ahead of the spectral plane, to the PPLN chip input facet for optimal waveguide coupling.

The PPLN poling period of 18.7 μm was chosen to support quasi phase-matched SFG between the signal and reference pulses' central wavelengths at a crystal temperature of 30°C, taking into account the increased effective refractive index in the slab waveguide region compared to that of bulk PPLN. The waveguide length of 4 mm in the light propagation direction and aperture of 10 mm in the spatial dispersion direction were chosen, respectively, to fully contain the focused spectral components' confocal length and the spatial extent of the dispersed light at the spectral plane.

The slab waveguide was fabricated by indiffusion of an 88 nm thick Ti layer at 1060°C for 8.5 h into the upper surface of the z-cut crystal. The intensity distribution of the waveguide mode at $\lambda \approx 1550$ nm is confined to approximately 3 μm FWHM in the vertical direction. This tight vertical confinement of the signal and reference beams results in increased intensity of the interacting light throughout the propagation length, enabling more efficient generation of SFG light. A broadband antireflection coating from 1500 to 1750 nm was deposited on the PPLN entrance facet and an antireflection coating at 810 nm on the exit facet. The PPLN was held at a temperature of 30°C (±0.1°C) for optimum phase matching.

The FWHM spot size of the focused spectral components within the crystal was approximately 14 μm. While the signal and reference beams coupled into the waveguide were confined in the vertical direction as single-mode guided waves, free-space diffraction of the focused spectral components in the nonguiding horizontal plane still limits the SFG interaction length. The confocal length in the horizontal direction was 1.2 mm; thus the full length of the chip is not exploited in practice; i.e., horizontal plane diffraction limits the maximum conversion efficiency achievable in our current experiment.

Note that the use of nondegenerate wavelengths for the interacting light is essential in order to avoid generation of strong background second-harmonic generation (SHG) light by the signal and reference pulses individually in the slab waveguide PPLN. This background light would propagate to the output plane and there degrade the pulse image quality, reducing the signal-to-noise ratio at the photodetector placed to receive the demultiplexed bit. The PPLN poling periodicity required for quasi phase-matched SFG between signal and reference beams with widely spaced wavelengths (i.e., 1550 and 1697 nm) does not allow for phase-matched SHG from the input wavelengths individually, and so the SHG background is negligible in this case.

Due to the matched yet flipped spatial dispersions of the two beams, noncritically phase-matched SFG between overlapping pairs of signal and reference spectral components at each point along the PPLN aperture results in a quasi-monochromatic output beam at 810 nm. A 75 mm lens coherently focuses the SFG light to the pulse image plane, with a 25 mm cylindrical lens used for vertical collimation of the light exiting the planar waveguide.

An example of a pulse image recorded by a CMOS camera at the image plane is shown, together with a Gaussian fit to its horizontal cross-section, in Fig. 3(a). The T-S

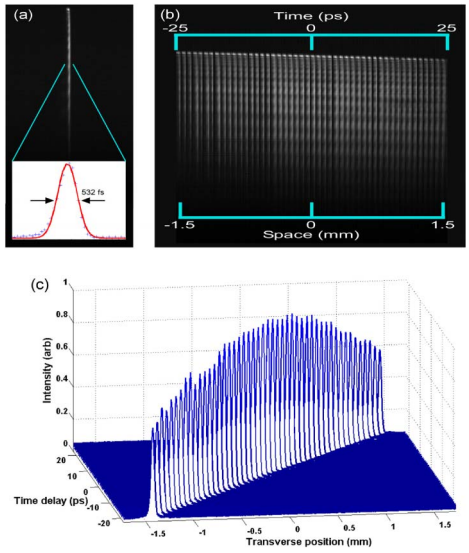

Fig. 3. (a) T-S converted signal pulse image with 532 fs FWHM, (b) 48 pulse images distributed throughout the T-S processor time window of 48 ps (composite image), and (c) pulse image intensity profiles showing shift in spatial position and intensity fall-off with increasing time delay.

conversion factor was measured as 62 μm/ps, by recording the shift in the transverse spatial position of the output pulse image at different signal pulse delay line lengths. This compares well with the calculated value of 59 μm/ps (see Ref. [15], where the Fourier lens focal lengths and diffraction grating frequency used are essentially the same as in the current experimental setup). The resulting FWHM pulse image width τ was found to be 532 fs, which is longer than the ideally expected image width of 232 fs corresponding to the cross correlation of a 100 fs signal pulse with a 210 fs reference pulse. We attribute this broadening to the poor beam quality of the reference beam ($M^2 = 1.3$). This results in less than optimal focusing of the reference pulse spectral components at the Fourier plane, reducing the T-S processor spectral resolution and so limiting the image plane resolution.

An important performance parameter of the T-S processor is the time window of operation ΔT. This is equivalent to the duration of the SFG output pulse and defines the maximum spatial extent of the T-S converted output parallel pulse images. The time window is determined by the temporal overlap of the interacting signal and reference pulses within the processor, which results in a drop in generated SFG signal power from the center of the time window toward its edges. The FWHM time window was measured as 48 ps by changing the delay line length and measuring the variation in SFG power.

The serial-to-parallel conversion factor N is defined as the time window ΔT divided by the pulse image width τ. This determines the maximum number of signal pulses that can be simultaneously demultiplexed by a single reference pulse to spatially separated parallel output channels. Our T-S conversion setup resulted in a conversion factor of $N = 90$. In order to demonstrate the potential for complete demultiplexing of a 1 Tbit/s OTDM channel, we recorded 48 individual pulse images at 1 ps separation throughout the FWHM time window [Figs. 3(b) and 3(c)]; it can be seen that there is clear spatial separation between adjacent output channels and the pulse images obtained are background free.

The T-S conversion efficiency η is defined as the SFG output power divided by the signal beam power coupled into the slab waveguide PPLN. We obtained a maximum conversion efficiency of 0.1% at 23 mW of coupled reference beam average power and a conversion efficiency slope of 4% per watt of coupled reference beam power [see Fig. 4]. Reference [13] reports a higher conversion efficiency of 0.6%; however, this was achieved at the expense of a reduced time window of 25 ps due to the decrease in spectral resolution required for fully exploiting the crystal interaction length (trading off efficiency for resolution).

The insertion losses for the signal and reference beams into the slab waveguide were measured as 4.1 and 4.9 dB, respectively. The average power and peak power of the signal (reference) beam at the PPLN waveguide entrance facet were 132 (70) mW and 16.5 (4.2) kW, respectively. Ideally, the pump power should be much higher than the signal power.

The SFG output signal bandwidth was measured as 0.1 nm (46 GHz) using light coupled via a multimode fiber into an optical spectrum analyzer [see Fig. 5]. This two-order-of-magnitude reduction from the input signal pulse bandwidth (from 5 THz to 46 GHz) implies the possibility for extraction of phase information from the converted signal by using coherent detection techniques.

The slab waveguide PPLN T-S conversion results are summarized and compared to those obtained with bulk PPLN [15] in Table 1. Note that the time window and serial-to-parallel resolution factors are similar for slab waveguide PPLN and for bulk PPLN T-S conversion. This is as expected since these parameters are determined

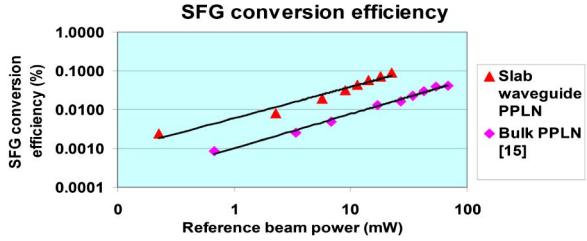

Fig. 4. T-S conversion efficiency slope for slab waveguide PPLN (red triangles) compared to our previous result with bulk PPLN crystal (pink diamonds; see Ref. [15]).

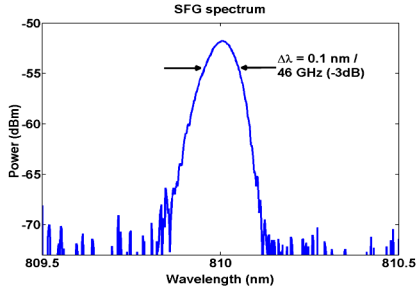

Fig. 5. Output SFG spectrum centered at 810 nm with a –3 dB bandwidth of 0.1 nm (= 46 GHz); the optical spectrum analyzer resolution was set to 0.01 nm for this measurement.

Table 1. Slab Waveguide PPLN and Bulk PPLN T-S Conversion Performance Parameters[a]

	ΔT (ps)	τ (fs)	N	η (%)	Conversion Efficiency Slope (%/W)	Bandwidth (nm)
Slab WG PPLN	48	532	90	0.1	4	0.1
Bulk PPLN [15]	42	440	95	0.03	0.6	0.09

[a]ΔT, FWHM time window; τ, FWHM pulse image width; N, serial-to-parallel resolution factor ($= \Delta T/\tau$); η, conversion efficiency. Note that due to insertion loss, the maximum conversion efficiency for the slab waveguide PPLN was obtained at lower reference beam average power (23 mW) compared to the bulk PPLN in Ref. [15] (64 mW).

solely by the spectral resolution of the dispersed signal and reference pulses at the spectral plane and ideally should not be affected by the type of nonlinear medium used. The principle difference between T-S conversion in the slab waveguide and bulk PPLN media is the conversion efficiency obtainable.

In summary, we have demonstrated T-S conversion of 100 fs pulses at 1.55 μm in a one-dimensional PPLN waveguide. This advance from a free-space nonlinear interaction to a semiguided wave regime resulted in increased SFG conversion efficiency, while maintaining high serial-to-parallel conversion resolution.

It should be noted that T-S conversion is a true serial-to-parallel demultiplexing technique, with all the signal pulses in the OTDM channel being simultaneously demultiplexed by a single reference pulse. In order to compare the optical power requirements of T-S conversion with other (single bit extraction) demultiplexing techniques, it is useful to consider the reference pulse energy-per-extracted-bit parameter. In our slab waveguide PPLN setup we use 3 pJ/bit to achieve 0.1% conversion efficiency. This compares with 1.1 pJ/bit for 0.8% conversion efficiency [5] and 1.7 pJ/bit for 0.06% conversion efficiency [6] for FWM single bit extraction in silicon and chalcogenide waveguides.

For high-bit-rate OTDM demultiplexing, for example, from 1 Tbit/s to 50×20 Gbit/s, our current slab PPLN waveguide T-S setup would require an average pump power of around 5 W. Clearly this is a higher than the acceptable pump power requirement for practical OTDM demultiplexing. In order to reduce the pump power, the T-S conversion efficiency could be increased by less tight focusing (in the horizontal direction) of the signal and reference spectral components, allowing for extended Rayleigh interaction range in a lengthened slab PPLN waveguide. This can be achieved by employing longer focal length lenses; however, this would increase the overall footprint of the system.

Finally, high-resolution T-S conversion may be exploited in a number of applications, including single-shot imaging of ultrashort temporal waveforms for investigating femtosecond time scale molecular dynamics and single wavelength channel photonically assisted analog-to-digital conversion, for which reference power is not a major concern, but having large conversion efficiency and signal strength are.

References

1. T. Richter, E. Palushani, C. Schmidt-Langhorst, R. Ludwig, L. Molle, M. Nolle, and C. Schubert, J. Lightwave Technol. **30**, 504 (2012).
2. B. C. Wang, V. Baby, W. Tong, L. Xu, M. Friedman, R. J. Runser, I. Glesk, and P. R. Prucnal, Opt. Express **10**, 15 (2002).
3. J. Du, Y. Dai, G. K. P. Lei, and C. Shu, Opt. Express **18**, 18691 (2010).
4. Y. L. Lee, H. Suche, Y. H. Min, J. H. Lee, W. Grundkotter, V. Quiring, and W. Sohler, IEEE Photon. Technol. Lett. **15**, 978 (2003).
5. F. Li, M. Pelusi, D.-X. Xu, A. Densmore, R. Ma, S. Janz, and D. J. Moss, Opt. Express **18**, 3905 (2010).
6. M. Galili, J. Xu, H. C. Mulvad, L. K. Oxenløwe, A. T. Clausen, P. Jeppesen, B. Luther-Davis, S. Madden, A. Rode, D.-Y. Choi, M. Pelusi, F. Luan, and B. J. Eggleton, Opt. Express **17**, 2182 (2009).
7. R. Takahashi, T. Yasui, J. Seo, and H. Suzuki, IEEE J. Sel. Top. Quantum Electron. **13**, 92 (2007).
8. E. Palushani, H. C. H. Mulvad, M. Galili, H. Hu, L. K. Oxenlowe, A. T. Clausen, and P. Jeppesen, IEEE J. Sel. Top. Quantum Electron. **18**, 681 (2012).
9. K. G. Petrillo and M. A. Foster, Opt. Express **21**, 508 (2013).
10. P.-C. Sun, Y. T. Mazurenko, and Y. Fainman, J. Opt. Soc. Am. A **14**, 1159 (1997).
11. A. M. Kan'an and A. M. Weiner, J. Opt. Soc. Am. B **15**, 1242 (1998).
12. D. M. Marom, D. Panasenko, P.-C. Sun, and Y. Fainman, J. Opt. Soc. Am. A **18**, 448 (2001).
13. J.-H. Chung and A. M. Weiner, J. Lightwave Technol. **21**, 3323 (2003).
14. D. Shayovitz and D. M. Marom, Opt. Lett. **36**, 1957 (2011).
15. D. Shayovitz, H. Herrmann, W. Sohler, R. Ricken, C. Silberhorn, and D. M. Marom, Opt. Express **20**, 27388 (2012).
16. D. Shayovitz, H. Herrmann, W. Sohler, R. Ricken, C. Silberhorn, and D. M. Marom, in *Conference on Lasers and Electro-Optics (CLEO 2013)*, OSA Technical Digest (online) (Optical Society of America, 2013), paper CTu3E.2.